

Ali ALAJMI, Hosny ABOU-ZIYAN, Hamad H. Al-MUTAIRI

# Reassessment of fenestration characteristics for residential buildings in hot climates: energy and economic analysis

© Higher Education Press 2021

**Abstract** This paper attempts to resolve the reported contradiction in the literature about the characteristics of high-performance/cost-effective fenestration of residential buildings, particularly in hot climates. The considered issues are the window glazing property (ten commercial glazing types), facade orientation (four main orientations), window-to-wall ratio (WWR) (0.2–0.8), and solar shading overhangs and side-fins (nine shading conditions). The results of the simulated runs reveal that the glazing quality has a superior effect over the other fenestration parameters and controls their effect on the energy consumption of residential buildings. Thus, using low-performance windows on buildings yields larger effects of WWR, facade orientation, and solar shading than high-performance windows. As the WWR increases from 0.2 to 0.8, the building energy consumption using the low-performance window increases 6.46 times than that using the high-performance window. The best facade orientation is changed from north to south according to the glazing properties. In addition, the solar shading need is correlated as a function of a window-glazing property and WWR. The cost analysis shows that the high-performance windows without solar shading are cost-effective as they have the largest net present cost compared to low-performance windows with or without solar shading. Accordingly, replacing low-performance windows with high-performance ones, in an existing residential building, saves about 12.7 MWh of electricity and 11.05 tons of CO<sub>2</sub> annually.

**Keywords** parametric analysis, high-performance window, window-to-wall ratio (WWR), facade orientation, solar shading, cost analysis

## 1 Introduction

The building sector worldwide consumed 36% of the total energy and released 39% of CO<sub>2</sub> in 2018, according to Energy Information Administration (IEA) [1]. The residential sector consumes 20% of all primary energy resources in the United States and about 30% of the European energy consumption [2]. In a severe hot climate, buildings are consuming over 70% of the total electricity generated [3], most of which by the residential sector. Consequently, the residential sector is considered the most pollutant sector. In such climates, it is a challenge to achieve a cost-effective net zero energy building (NZEB). It is well recognized that the best practice to establish NZEB is to minimize its energy consumption to the lowest possible to be able to cover it by the generated renewable energy annually [4,5]. Thus, applying passive design strategies is essential to minimize energy consumption and attain cost-effective NZEB [6,7]. This is confirmed by the fact that the implementation of some passive design strategies to an envelope of the residential building shows energy savings between 39.5% and 47.3% [8]. The appropriate building facade (the facade orientation, window-to-wall ratio (WWR), window properties, shading elements, and wall insulation) is vital to recognize a cost-effective low-energy building [9,10].

With the continuous development in the building wall materials including phase-change insulation [11–13] and reflective paint (with a solar reflectivity of up to 98%), the building fenestration is considered the weakest thermal component in the building envelope. This is confirmed by the fact that it is responsible for as much as 60% of the total energy consumption of a building because the fenestration overall heat transfer coefficient is up to five times greater than other components of the building envelope in addition

Received Jan. 22, 2021; accepted Aug. 23, 2021; online Jan. 10, 2022

Ali ALAJMI, Hamad H. Al-MUTAIRI  
Mechanical Engineering Department, College of Technological Studies,  
PAAET, Kuwait

Hosny ABOU-ZIYAN (✉)

Mechanical Engineering Department, College of Technological Studies,  
PAAET, Kuwait; Mechanical Power Engineering Department, Faculty of  
Engineering, Helwan University, Cairo, Egypt  
E-mail: hz.abouziyan@paaet.edu.kw

to the solar radiation transmitted through it [14]. Thus, a careful design of the fenestration characteristics such as facade orientation, window size (or WWR), number of glazing panes, glass properties, window framing, and solar shading devices plays a major role in controlling the heating and cooling loads in the building. However, there are some contradictions in the literature about the fenestration characteristics as reported in the following discussion.

The effect of facade orientation on energy consumption in severe cold regions indicated that the lowest energy is on the north facade followed by the south and the east (west) orientation [15]. However, the ratio of heat gain or loss through the window varies by roughly a factor of 30 depending on the glazing quality and the facade orientation [16]. Rotating the main facade from the south direction may decrease the effect of glazing properties by 0%–24% [17]. In a tropical climate of the northern hemisphere, the heat gain through the southern shaded windows is the most optimal for the annual conditioning load, followed by east, west, and north-facing windows [18]. Many studies were focused on windows in the south facade only [19–22]. Although the discussed results showed the significant effect of the facade orientation on energy consumption, a contradiction on the best facade orientation between results on the cold [15] or warm climate [18] still existed in the literature [22], possibly due to the interaction of other effects of glazing properties or solar shading.

The effect of window size or a WWR received considerable attention in the literature. A series of investigations [19–21] with different wall  $U$ -values indicated that the optimal WWR for walls with very low  $U$ -values was smaller than that for walls with higher  $U$ -values. Another study on intermediate floors in residential buildings concluded that the total annual heating load decreased in a cold climate and increased in a warm climate as the south window size of apartments was increased [22]. Additionally, the influence of the WWR of 16%–41% on the required heating and cooling energy and peak loads in Italy showed that the window size had less influence during winter but had a considerable effect during summer [23]. Another study on a single-story house in Jordan and Germany indicated that the heating load was highly sensitive to windows type and size as compared with the cooling load [24]. In summary, similar conclusions are reached in Refs. [16,24], which are opposite to that reported in Ref. [24] whereas other studies related the effect of window size to the  $U$ -value of the wall [19–21]. In addition, the conclusion reached in Ref. [22] is limited to the heating load only and was subjected to climate conditions.

The effect of glazing specification on the heating and cooling loads was investigated using single, double, and triple low- $e$  glazing window types. Two different triple glazing windows were tested in Refs. [16,17] and single triple glazing in Refs. [18–20] with a solar heat gain

coefficient (SHGC) of 0.52 and a  $U$ -value of 0.51  $W/(m^2 \cdot K)$ . It should be stated that the work in Refs. [16–20] tested the limited optical properties of the glazing material. As discussed earlier, the glazing quality affected the energy consumption in buildings considerably [16] and that effect decreased as the facade orientation was shifted from the south direction [17]. The thermal transmittance of the glazing affected energy and peak loads considerably in both winter and summer seasons [23]. On the contrary, the results reported in Ref. [24] indicated that the heating load was highly sensitive to the type of windows compared with the cooling load, and that with a well-optimized glazed window, the energy-saving could reach 20%–24% [24]. Reducing the cooling load of the building with five different commercial glazing types indicated that the SHGC was a more dominating factor than the  $U$ -value [25]. Based on a life-cycle cost analysis, it was found that windows with double low- $e$  clear filled with argon gas were the most cost-effective for residential buildings in South Korea [26]. Nevertheless, windows with triple low- $e$  glazing provided the highest energy savings and carbon reductions but were not cost-effective [27]. In conclusion, double low- $e$  glazing was a cost-effective window compared to the triple low- $e$  glazing one. However, a limited range of glazing properties was examined in the reported literature and a contradicted conclusion on the significance of window quality on the cooling loads still existed [23,24].

The effect of solar shading on energy consumption in a hot climate showed that considerable savings could be achieved by light shelf photovoltaic of office buildings [28,29]. In a typical residential building in Iran [30], the results on all main orientations showed that appropriate overhangs or side fins in the south, west, and east windows would lead to the optimal reduction of the annual energy transferred into the buildings and could have a competitive performance to high-performance glazing. However, only limited window types were tested. Additionally, the influence of the depth ratio and perforation percentage of the external fixed deep wooden solar screens in a residential building in a hot and arid desert climate (El-Kharga Oasis, Egypt), was considered [31]. The results indicated that the optimal solar screens were more efficient than the traditional ones as they could achieve energy savings of up to 30% of the annual energy loads in the south and west orientations. On the other hand, the results in a high-rise residential building in Singapore showed that the half egg-crate louver was most suitable for the southern and northern facades, whereas a horizontal projection (overhang) was most appropriate for the eastern and western facades [32]. The effect of louver inclination angle, louver-to-window area ratio, and window orientation on the cooling and heating loads for a residential building showed that the cooling load was decreased when the optimal window parameters were used [33]. In conclusion, the effect of solar shading on building energy

consumption depends on the facade orientation, and glazing quality. However, the quantitative effect of those parameters on the shading devices needs to be identified and explored.

Based on the above discussion, appropriate fenestration characteristics (facade orientation, windows size, glazing quality, and solar shading) constitute a pivotal role in controlling energy consumption in a residential building. However, many contradictions regarding the best facade characteristics still appear in the literature. For example, many studies concluded that the north facade was the best [15] whereas others challenge their conclusion [19–21]. Besides, the effect of glazing properties was not comprehensively considered [17–20] as neither the best facade orientation nor solar shading requirement was assessed in terms of window glazing properties. In addition, many studies only concentrated on a single design parameter, ignoring the interaction with the other fenestration characteristics [26,27]. Moreover, most of the work was conducted using the optimization approach that provided an optimum solution to satisfy the objective functions [34]. However, the parametric analysis has the advantage of exploring the quantitative effect of each design variable. Finally, most of the reported work was conducted on the European climate without considering the cost analysis or lighting energy in hot climate countries. Therefore, settling the contradictions that existed in the literature about the characteristics of residential building fenestration in a hot climate need to be considered.

In the present work, a residential house in a severe hot climate was considered with the aim to investigate the contradicted fenestration characteristics thoroughly. First, an optimization approach using the genetic algorithm (GA) integrated with EnergyPlus [35] was applied to identify the influential design characteristics of the fenestration. All design parameters of windows were considered, and the outcome solutions were analyzed to identify the main design parameters affecting heating, cooling, and lighting energy consumptions. The facade orientation (east, west, north, and south), glazing quality (ten different double glazing types with a wide range of properties including SHGC (0.20–0.85),  $U$ -value (1.15–3.40), and light transmission (LT) (0.21–1.0)), window size (WWR of 0.2–0.8 with a step of 0.1), overhang projection (0, 0.25, and 0.50 of window height), and side-fin projection (0, 0.25, and 0.50 of window width) were identified as the main design parameters. In addition, a parametric study of the main design parameters was conducted on the derived 2520 possible solutions to elaborate on the effect of each considered design parameter on the energy consumption of the building. Moreover, the best facade orientation and the significance of solar shading requirements were assessed and correlated in terms of window glazing properties. Furthermore, a cost analysis was performed to evaluate the cost-effectiveness of different window glazing specifications or various cases of shading devices. This paper

provides answers to many contradictions about the facade characteristics and affords the building designers with practical passive strategies to achieve the best fenestration design and facilitate NZEB design in a severe hot climate.

---

## 2 Research method

Two approaches were suggested to conduct the present work, the optimization technique and the parametric study. The simulation-based optimization approach links a building simulation program (EnergyPlus) and an GA in energy simulation [36]. It has been proven to be computationally efficient [37] to identify the optimal solutions for the specified criteria. On the other hand, the parametric study is a comprehensive research method simulating all possible design combinations from a discrete search space [38]. It is computationally intensive, but more suitable for creating design guidelines [39,40]. In such a method, the effect of each design parameter, in the full solution space, can be explored and an appropriate design may be approached [40]. The parametric study may incorporate sophisticated sensitivity analysis techniques [41] for building thermal simulations. Some sensitivity techniques change only one parameter at a time, keeping other input parameters constant [42]. Other sensitivity techniques may use the sampling techniques such as the Monte Carlo method to investigate multiple inputs while simulating only some of the total possible design combinations [38,39,42]. These methods prove especially valuable when computing power is limited, or the set of possible combinations is very large.

It is worth noting that the present work was first conducted using the optimization approach with a full list of fenestration design parameters. The analysis of the obtained optimization solutions indicated that some variables were fixed in all optimized solutions (window frame and dividers materials, room zone depth, and daylighting sensor location), other variables were less important such as overhang tilt angle, and the rest is the most important input parameters. Then, the parametric study was conducted on the important design parameters to investigate their effect on the light and total energy consumption of the tested room. It has been found that using the same inputs with the same increments, both optimization and sensitivity approaches yield the same optimum solution that satisfies the minimum annual energy consumption and the maximum use of daylighting (minimum artificial lighting energy). In this paper, however, the results are presented using the parametric analysis approach.

### 2.1 Local weather data

Kuwait is situated in the north-east of the Arabian Peninsula, at a latitude of 29°22' north and a longitude of

47°58' east. The summer season spreads over long months from April to October when the temperature could reach as high as 50°C in July and August with a low humidity; and in the cold season, from November to March, the temperature ranges between 5°C and 25°C with a considerable relative humidity. The cooling degree of Kuwait is around 3442 h, based on 18.3°C [43]. The high temperature of the local weather and its long summer season lead to a high energy demand, which may peak in July and August due to the need for a nonstop air-conditioning system [44].

Coincidentally, Kuwait and other gulf council countries (GCC) get the highest solar irradiance in the world [45]. The average hourly global solar radiation is 440 Wh/(m<sup>2</sup>·h) for nine hours of sunshine per day. Figure 1 shows the main weather elements (temperatures and solar radiation) of a typical year in Kuwait. The hourly weather data including dry-bulb temperature, dew point temperature, solar radiation, wind speed, and direction are required by the computer simulation software. Since weather conditions can vary significantly from year to year, there is a need to derive the typical meteorological year (TMY) data to represent the long-term typical weather condition over a year [46].

## 2.2 Building simulation program (EnergyPlus)

This new generation building energy simulation program is the outcome of more than two decades of developments by the US Department of Energy [47]. The thermal model calculation is based on a non-steady-state conducted for the entire year on an hourly basis. The heat transfer equations of conduction, radiation, and convection were used, which allowed robust thermal performance predictions. EnergyPlus links the outdoor conditions using weather data, which is based on the TMY weather format with the specified indoor conditions. In this study, the

indoor temperatures were set at 21°C and 24°C for the winter and summer seasons, respectively. The temperature setpoints are for the theoretical study with the purpose to simplify the problem to some extent. Indoor heat loads such as equipment and occupants were assumed to be constant to observe the impact of the fenestration design parameters on the heat flow.

In this study, the ideal load template available in EnergyPlus used “HVAC (Heating Ventilation and Air Conditioning) Template: Zone: Ideal Loads Air System” to calculate the required heating, and cooling demands on each calculating step for the zone with a design factor of 1.25 for heating and 1.15 for cooling. Numerous research projects validated the performance and accuracy of EnergyPlus [48].

## 2.3 Simulation setup program (Java EnergyPlus (jEPlus))

Parametric analysis is a powerful method for realizing alternative design parameters in order to explore their effect on a certain goal such as minimizing energy consumption. Generating many building simulations requires an automated approach to simplify such a process. This is accomplished using the jEPlus program, which takes the advantage of the text-based user interface of EnergyPlus to make it a perfect automated (or scripted) simulation tool. Since the number of simulations required for parametric analysis tends to be large, “Parallelism” is a software utility that is another competitive advantage [49,50].

## 3 Studied zone model

### 3.1 Zone model description

The space analyzed in this study is a living room having

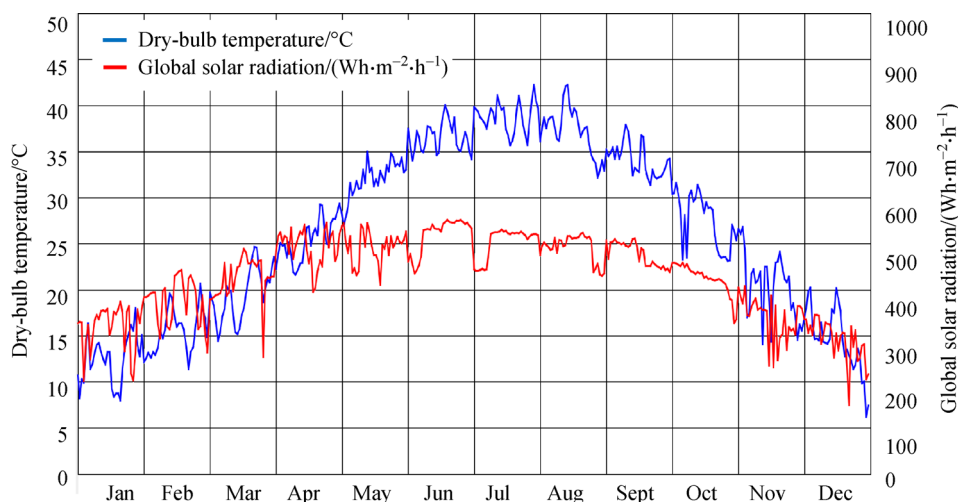


**Fig. 1** Dry-bulb temperature and average hourly global solar radiation in Kuwait.

internal dimensions of  $4\text{ m} \times 4\text{ m} \times 4\text{ m}$ , as demonstrated in Fig. 2. The room is on the middle floor and its facade is changed to one of the four main orientations (east, west, north, and south). Therefore, only the facade changes heat with the surroundings while the other internal walls, roof, and floor are assumed adiabatic.

### 3.2 Investigated design parameters

The design parameters need to be carefully selected to avoid excessive computational time. Based on the outcome of the optimization solutions in this study, five significant design parameters are identified and listed in Table 1. The representative room facade may be oriented in the east, west, north, or south direction. The WWR was varied from 0.2 to 0.8 with a step of 0.1 where the minimum WWR of 0.2 ensured adequate view to the outside and the maximum WWR was restricted to 0.8 to limit the negative impact of excessive solar penetration in the forms of heat and glare. For the number of window glazing panes, a double-glazing window was used as it proved to be the most cost-effective window [27] and presented the common practice construction for residential buildings. Ten different commercial glazing materials were chosen to investigate the effect of glazing quality. Those glazing materials represent the common types in the local market where their specifica-

tions vary from the classical transparent (double clear) glazing to the energy-efficient (low-e) glazing, as listed in Table 2. Additionally, the overhang projection ( $P$ ) was set as 0, 0.25, and 0.50 of the window heights ( $H$ ) with a fixed tilt angle of  $90^\circ$  (horizontal). Finally, the side-fins projection ( $F$ ) was chosen to be 0, 0.25, and 0.50 of the window widths ( $W$ ). These design parameters permute 630 possible solutions (search space) for each facade orientation and a total of 2520 solutions for the four orientations.

### 3.3 Other input parameters

The other input parameters that are not specified in Section 3.2 and incorporated in the EnergyPlus model are listed in Table 3. These inputs were used to obtain the cooling load for the room that represented the most active energy in a residential building. These parameters were considered in obtaining the baseline cooling load for all solutions. The building is of heavy construction type, which is the common practice in such hot climate, (refer to the  $U$ -values for walls and roof in Table 3).

### 3.4 Daylighting and lighting interaction

The amount of natural lighting (daylight) that is penetrating a space is influenced by many factors including sky

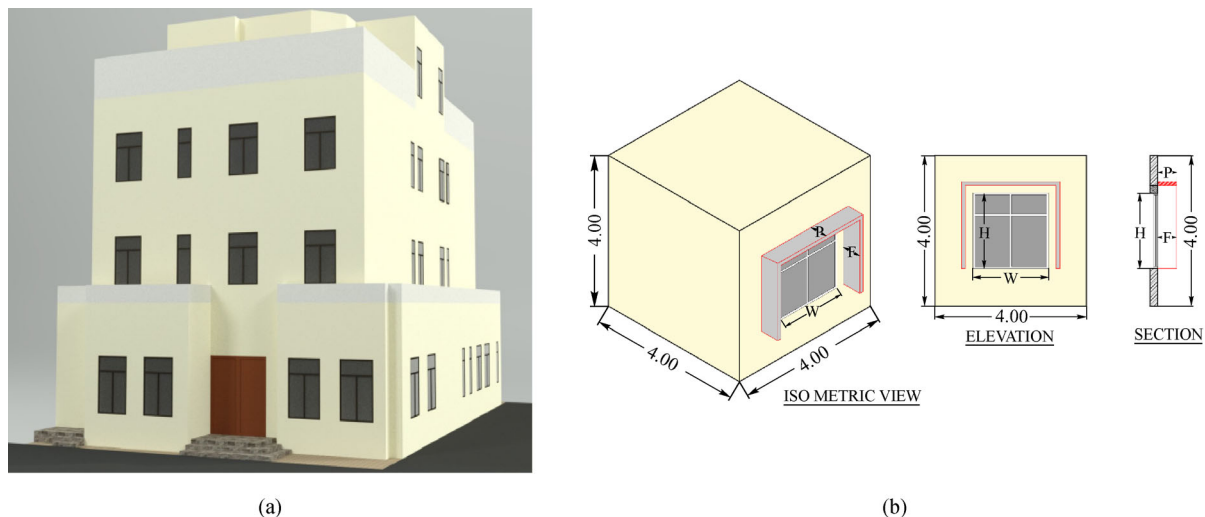


**Fig. 2** Zone model and computational domain description.

(a) Typical house in Kuwait; (b) computational domain (isometric, elevation, and section views of the studied living room; refer to Tables 1–3 for the investigated parameters and boundary conditions).

**Table 1** Investigated design parameters

Index	Variable	Type	Lower bound	Upper bound	Initial value	Increment
1	Facade orientation	Discrete		(east, west, north, and south)		
2	WWR/%	Discrete	0.2	0.8	0.2	0.1
3	Glazing quality (see Table 2)	Discrete	W1	W10	W1	1
4	Overhang projection ( $P$ )	Discrete	0	0.50 $H$	0.00	0.25
5	Side-fins projection ( $F$ )	Discrete	0	0.50 $W$	0.00	0.25

**Table 2** Double glazing window specifications

No.	Configuration	SHGC	$U/(W \cdot m^{-2} \cdot K^{-1})$	LT	Cost/(USD $\cdot m^{-2}$ )	Cost difference	Window quality
W1	Low-e double sliver (6 mm-12 mm-6 mm) air	0.20	1.60	0.28	53	23	
W2	High performance (8 mm-16 mm-8 mm) xenon	0.22	1.23	0.21	67	37	High
W3	Low-e neutral (8 mm-16 mm-8 mm) xenon	0.26	1.40	0.40	67	37	
W4	Low-e neutral blue (6 mm-12 mm-6 mm) air	0.31	1.60	0.50	53	23	
W5	Super low-e neutral (6 mm-12 mm-6 mm) xenon	0.37	1.15	0.50	73	43	Medium
W6	Low-e super neutral (6 mm-12 mm-6 mm) air	0.38	1.60	0.69	57	27	
W7	Low-e clear (6 mm-16 mm-6 mm) argon	0.56	1.52	0.76	67	37	Low
W8	Reflective (6 mm-8 mm-6 mm) air	0.64	1.99	0.76	30	0	
W9	Clear (6 mm-4 mm-6 mm) air	0.74	3.40	1.00	30	0	
W10	Clear (6 mm-6 mm-6 mm) air	0.85	3.06	0.8	30	Base	

**Table 3** Fixed design parameters of the tested room

Characteristics	Description of the studied case
Wall $U$ -value without thermal bridge/( $W \cdot m^{-2} \cdot K^{-1}$ )	0.574
Roof $U$ -value/( $W \cdot m^{-2} \cdot K^{-1}$ )	0.397
Occupancy density of the tested room/( $m^2 \cdot person^{-1}$ )	4
Lighting load/( $W \cdot m^{-2}$ )	5
Equipment load/( $W \cdot m^{-2}$ )	3
Ventilation/( $L \cdot s^{-1} \cdot person$ )	10
Infiltration/Air change (ACH)	0.5
Thermostat setting/ $^{\circ}C$	24 in summer and 21 in winter
Illuminance level/( $Lux \cdot m^{-2}$ )	300
Glare maximum allowable index	19
Frame material of the window/( $W \cdot m^{-2} \cdot K^{-1}$ )	5.881 (polyvinyl chloride (PVC))
Window divider/( $W \cdot m^{-2} \cdot K^{-1}$ )	5.881 (PVC)
Occupancy/Lighting/Equipment schedules	Schedule: Time, active fraction Weekdays: 00: 00–12: 00, 0; 12: 00–14: 00, 0.5; 14: 00–18: 00, 1; 18: 00–24: 00, 0.5 Weekends: 00: 00–12: 00, 0; 12: 00–13: 00, 0.5; 13: 00–23: 00, 1; 23: 00–24: 00, 0.5 Note: 0 = zero, 0.5 = half, and 1 = All

condition, sun position, location, window size, window glass transmittance, window shades, and reflection of interior surfaces. Building simulation programs such as EnergyPlus considers all these factors in the calculation of the daylighting illuminance. In EnergyPlus, many objects can be used to handle the interaction between daylight and artificial light. In this work, an advanced object (Daylighting: LightFlux) is used with the building example. A reference point is set in the middle of the room (2 m from the window side) to trigger the lighting system based on the illuminance level (300 Lux) at this point. This reference point ensures the balance between adequate illuminance and energy consumption. Practically, photocells would be integrated with the electrical lighting system that controls the lighting illuminance level based on the response to the daylight illuminance levels at the specified reference point.

### 3.5 Glare index

The considered maximum allowable glare index, for living activity when the occupant is viewing  $90^{\circ}$  from the light source, is 19. The glare index at the reference point is calculated using the following equations [51]:

$$G(i_L) = 10 \log \sum_{\substack{\text{windows} \\ \text{in zone}}} \frac{S_w(i_L, i_S)^{1.6} \Omega(i_L)^{0.8}}{B(i_L) + 0.07 \omega(i_L)^{0.5} S_w(i_L, i_S)}, \quad (1)$$

$$B(i_L) = \max\{B_w(i_L), \rho_b, J_{\text{set}}(i_L)\}, \quad (2)$$

where  $i_L$  and  $i_S$  are reference point index and window shade index;  $S_w$  and  $B_w$  are the window luminance ( $cd/m^2$ )

and window background luminance ( $\text{cd/m}^2$ );  $\omega$  is the solid angle subtended by the window with respect to the reference point (steradians),  $\Omega$  is the solid angle subtended by the window, modified to take the direction of occupant view into account (steradians);  $\rho_b$  is the area-weighted average reflectance of zone interior surfaces; and  $I_{\text{set}}$  is the illuminance setpoint ( $\text{cd/m}^2$ ), which will balance with the other inputs units. In Eq. (2), the background luminance is approximated as the larger of the background luminance from daylight and the average background luminance that would be produced by the electric lighting at full power if the illuminance on the room surfaces is equal to the setpoint illuminance. In a more detailed calculation, where the luminance of each room surface is separately determined,  $B(i_L)$  would be better approximated as an area-weighted luminance of the surfaces surrounding a window considering the luminance contribution from the electric lights.

#### 4 Cost analysis of window types

Economic assessment of window types with and without solar shading can strongly influence the final selection of the window type, size, and attached shading. Accordingly, the cost analysis study presents a detailed economical evaluation based on a 30-years financial plan for the considered windows. For the scenario without solar shading, the study is based on the annual saving of electrical energy using windows (W1–W9) if the base case window (W10) is used. For the second scenario with solar shading, the annual saving is based on the difference between the consumption using the window itself with and without shading. Hence, it is very important to estimate the initial and future values of associated cash flows (CFs) during the intended period for the scenarios with and without solar shading. It is to be indicated that the cost listed in Table 2 is for glass only and the frame cost is not considered as it is fixed for a certain WWR for all window types.

The cost analysis study considers the initial payments of cash associated with the glazing cost (GC) of the window, solar shading (overhang, and side fins) costs (SSC). Those costs are paid during the building installation and estimated at the market price today. But long-term economic evaluation is subjected to changes in prices and other economic factors. For this reason, it is very essential to estimate other CFs associated with the studied scenarios in present value (PV). In this regard, the study assumes that there will be no specific recurring cash to be paid by the house owner. However, there is an annual amount of cash that results from electrical energy saving acquired by window glazing and solar shading. Based on that, those amounts of annual cash savings are considered as annual returns, which must be calculated in PV.

The PV method depends on the time equivalent value of

past, present, or future CFs as of the beginning of the base year [52]. CF is subjected to future discount rate ( $r$ ) occurrence period ( $n$ ) as shown in Eq. (3).

$$\text{PV} = \frac{\text{CF}_1}{(1+r)^1} + \frac{\text{CF}_2}{(1+r)^2} + \frac{\text{CF}_3}{(1+r)^3} + \dots + \frac{\text{CF}_n}{(1+r)^n} \text{CF}_i, \quad (3)$$

where  $\text{CF}_i$  presents the annual electrical energy savings, the discount rate  $r$  is estimated to be 1.5% according to recent local financial data, and the studied period  $n$  is 30 years. The CF from saved electrical energy for the various windows is calculated based on the amount of annual electrical energy consumption difference between each studied window and window 10. Selecting this window as a benchmark for the evaluation is explained by its high energy consumption compared to the other windows. In addition, it is the existing window in most residential buildings. Therefore, the study intends to illuminate the significance of choosing a better glazing type of window instead of the present window (W10) due to its low initial price. In the case of using solar shaded windows, electrical energy saving is the difference between the annual energy consumption for the same window with and without solar shading. Thus, the CF from saved electrical energy related to this benchmark is given in Eq. (4).

$$\text{CF} = (E_{w10} - E_{wi}) \times \text{PC}, \quad (4)$$

where  $E_{w10}$  and  $E_{wi}$  present the annual electrical energy consumed by the room using W10 and other windows (W1–W9) and the production cost of electrical energy (PC) presents the production cost of electrical energy in Kuwait, which is estimated at 0.126 USD/kWh [53]. Thus, the entire CFs are presented in terms of net PV without solar shading ( $\text{NPV}_{\text{wt}}$ ) and with solar shading ( $\text{NPV}_{\text{ws}}$ ), as given in Eqs. (5)–(6).

$$\text{NPV}_{\text{wt}} = -\text{GCD} + \sum_1^n \frac{\text{CF}_n}{(1+r)^n}, \quad (5)$$

$$\text{NPV}_{\text{ws}} = -\text{SSC} + \sum_1^n \frac{\text{CF}_n}{(1+r)^n}. \quad (6)$$

The initial cost difference between window GC and window 10 GC (GCD) presented in Eq. (5) is calculated as the extra cash that is supposed to be paid for choosing windows from W1 to W9 compared to window 10 as listed in Table 2. The costs of window glazing, overhang projections, and side fins are based on local market prices in Kuwait. For the SSC, it is expected to be made of aluminum whose price is estimated at 83 USD/m<sup>2</sup> based on prices obtained from a local fabricator. The simple payback period (SPP) for the cases of windows without and with solar shading is calculated using Eqs. (7) and (8),

respectively.

$$SPP_{wt} = \frac{GCD}{CF}, \quad (7)$$

$$SPP_{ws} = \frac{SSC}{CF}. \quad (8)$$

## 5 Results and discussion

The results of the annual heating, cooling, and lighting energy consumptions of the tested room for the alternative combinations of seven WWRs (0.2–0.8 with a step of 0.1), ten window types, and nine different conditions of overhang and side-fins shading devices are tested. Those combinations provide 630 possible solutions in each facade orientation, giving a total of 2520 cases in the four main orientations. It is worth noting that the simulation runs are ensured not to violate the thermal comfort, which is indicated by the predicted mean vote thermal occupant's comfort index (PMV) of  $-0.5$  to  $0.5$ .

Before conducting the parametric study of the present work, it is essential to confirm that the energy consumption of the considered building produced by the present model lies within the recognized values of similar residential buildings in a hot climate. Therefore, the results were validated using the energy use intensity (EUI) as a commonly used building energy performance indicator. EUI is measured by dividing the total annual energy consumption of a building by its total floor area. The average EUI of a typical residential house (Villa) ranges from 164 to 247 kWh/(m<sup>2</sup>·a) [54] depending on the facade orientation and WWR using a window like W10. The obtained EUIs of the considered building using W10 and WWR of 0.2–0.5 are 176.1–208.5 kWh/(m<sup>2</sup>·a) for the north, 177.5–226.2 kWh/(m<sup>2</sup>·a) for the south, and 186.8–237.6 kWh/(m<sup>2</sup>·a) for the east and west facades. Therefore,

the predicted EUIs using the present model agree with the EUIs reported in Ref. [54].

### 5.1 Combined effects of fenestration parameters

The 630 combinations of WWRs, window types, and shading conditions in each facade provide the scattered data of the annual energy consumption (on the  $y$ -axis) and artificial lighting energy (on the  $x$ -axis). Since the data patterns for east, west, and south facades are similar, two facades are presented in Figs. 3(a) and 3(b) for the east, and north facades, respectively. The results in each facade are categorized according to the WWR where each category contains 90 cases for ten window types and nine different shading conditions. Similar energy consumption trends in the room are observed for the various facades. In general, the energy consumption (heating and cooling) of the room varies from about 2590 to over 4500 kWh (74% or higher) for east, west, and south facades and from 2553 to 3841 kWh (about 50%) for the north facade. Thus, the north facade room requires lower energy than rooms in the other facades.

Also, the energy required for artificial lighting consumption starts from about 190 for all facades to 202 kWh (6%) for the west facade, 220 kWh (16%) for the south facade, and around 240 kWh (26%) for the east and north facades. Therefore, the rooms in the east facade receive more daylighting and require lower energy for artificial lighting than other facades. The lighting consumption represents 4.06% to 9.46% of the total energy consumption in residential buildings. Unexpectedly the maximum lighting consumption occurs at WWR of 0.3, not 0.2 (Figs. 3(a) and 3(b)).

Figure 4 illustrates part of the results, shown in Fig. 3 in the two facades, for two specific WWRs, i.e., 0.2 (Figs. 4(a), and 4(c)) and 0.8 (Figs. 4(b) and 4(d)). Those two WWRs are chosen to explore the contribution of window types and shading conditions on the smallest and

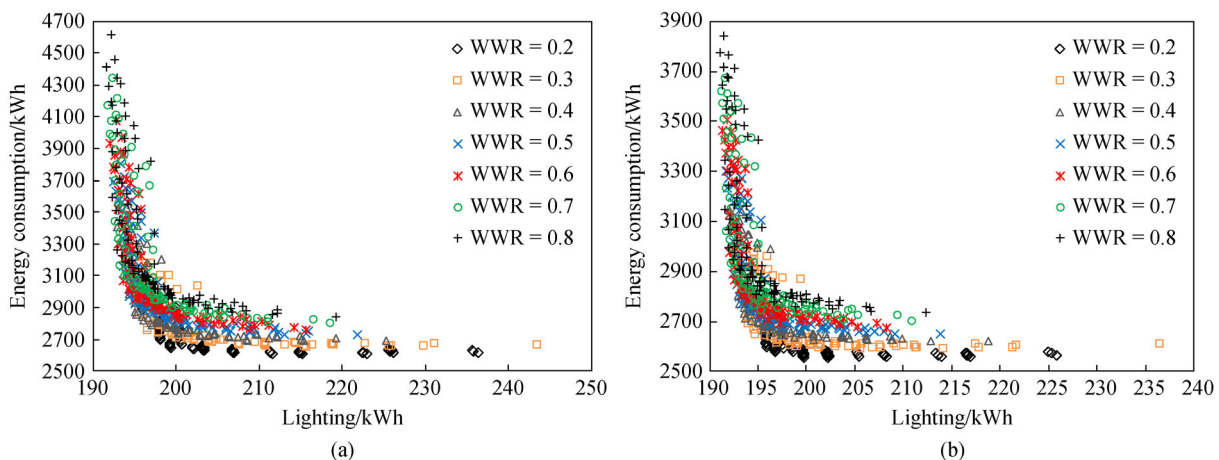


**Fig. 3** Possible solutions at different design parameters. (a) East facade; (b) north facade.



largest considered WWRs. The results for each WWR contain ten window types where each one has nine different shading cases, which include full overhang and/or side-fins, half overhang and/or side-fins, and no overhang and/or side-fins.

Figure 4 exhibits similar trends of the results in all facades for either WWR of 0.2 or 0.8. The energy consumption of the room increases, and the lighting consumption decreases as the WWR increases. Besides, the room energy consumption of the north facade is lower than that of the east facade, particularly for the large WWR. The energy consumption of WWR of 0.8 varies from 2843 to 4618 kWh, in the east facade, i.e., about 62% variation in the energy consumption of the room as a result of implementing different window types and shading devices. Moreover, there are cases for W1–W3 at WWR of 0.8 that have a lower energy consumption than other windows (W4–W10) at WWR of 0.2, in the four facades. These observations indicate that with the proper use of window types and shading devices, large windows with a WWR of up to 0.8 may consume energy lower than an improper window specification with a WWR of 0.2 (Fig. 4). In conclusion, the wide variations of energy consumption and artificial lighting energy, in Figs. 3 and 4 indicate the significant influence of the fenestration design parameters such as facade orientation, WWR, window

type, and shading conditions on total and lighting energy consumption.

## 5.2 Effect of design parameters on unshaded fenestration

### 5.2.1 Annual energy consumption

The preceding section discusses the combined effect of facade orientation, WWR, window type, and shading devices on the tested room energy consumption. However, a further insight analysis is necessary to quantify the effect of each fenestration parameter, under different conditions, so that a better design of high-performance fenestration for low or zero-energy buildings can be achieved.

The annual energy consumption of the room using either of the considered ten windows without the use of an overhang or side-fin solar shading is illustrated in Figs. 5(a)–5(d) when the tested room facade is located in the east, west, north, or south, respectively, for WWRs of 0.2, 0.4, 0.6, and 0.8. The four frames in Fig. 5 are plotted with the same range of energy consumption on the y-axis to ease the visual comparison between the four facades.

Figure 5 depicts large variations in room energy consumption with window types, WWRs, and facade orientations. According to energy consumption, the windows may be classified as high-performance windows

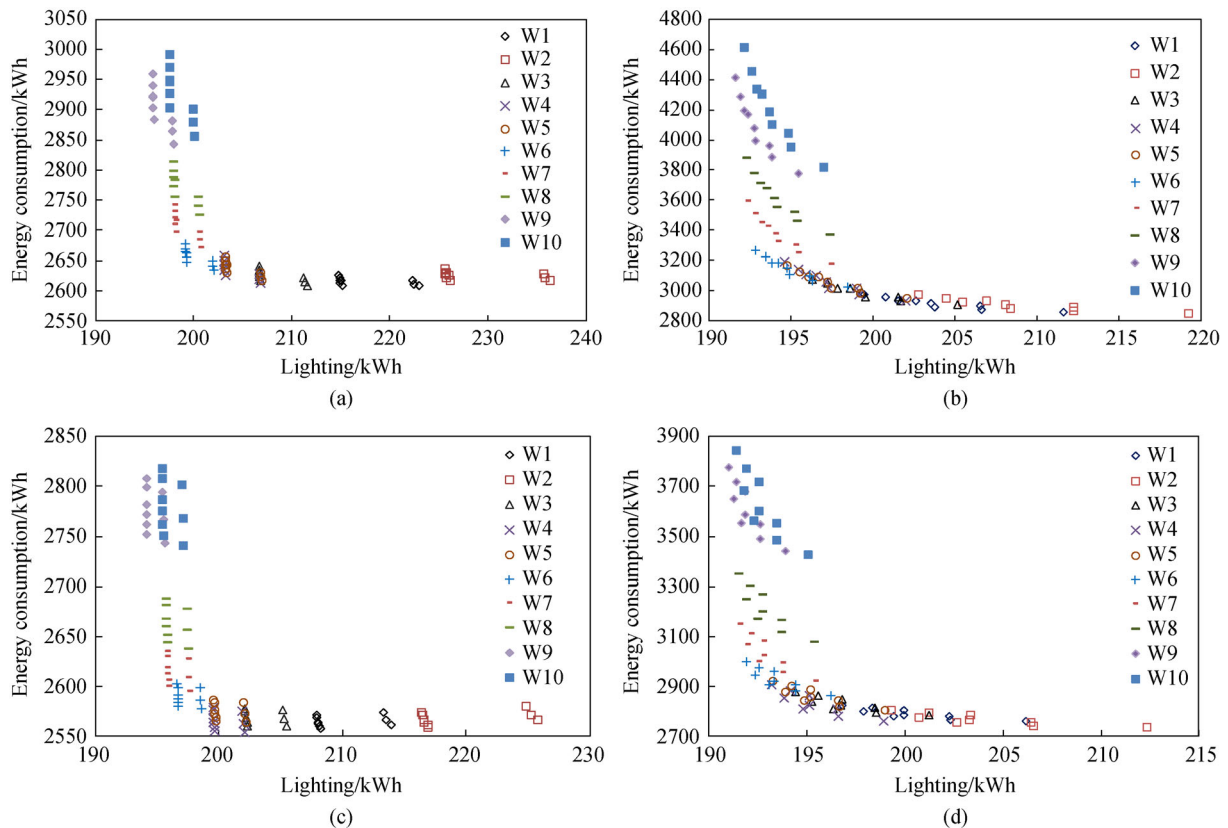


**Fig. 4** Alternative possible solutions for window conditions in east and north facades at WWRs of 0.2 and 0.8.  
 (a) East, WWR = 0.2; (b) east, WWR = 0.8; (c) north, WWR = 0.2; (d) north, WWR = 0.8.

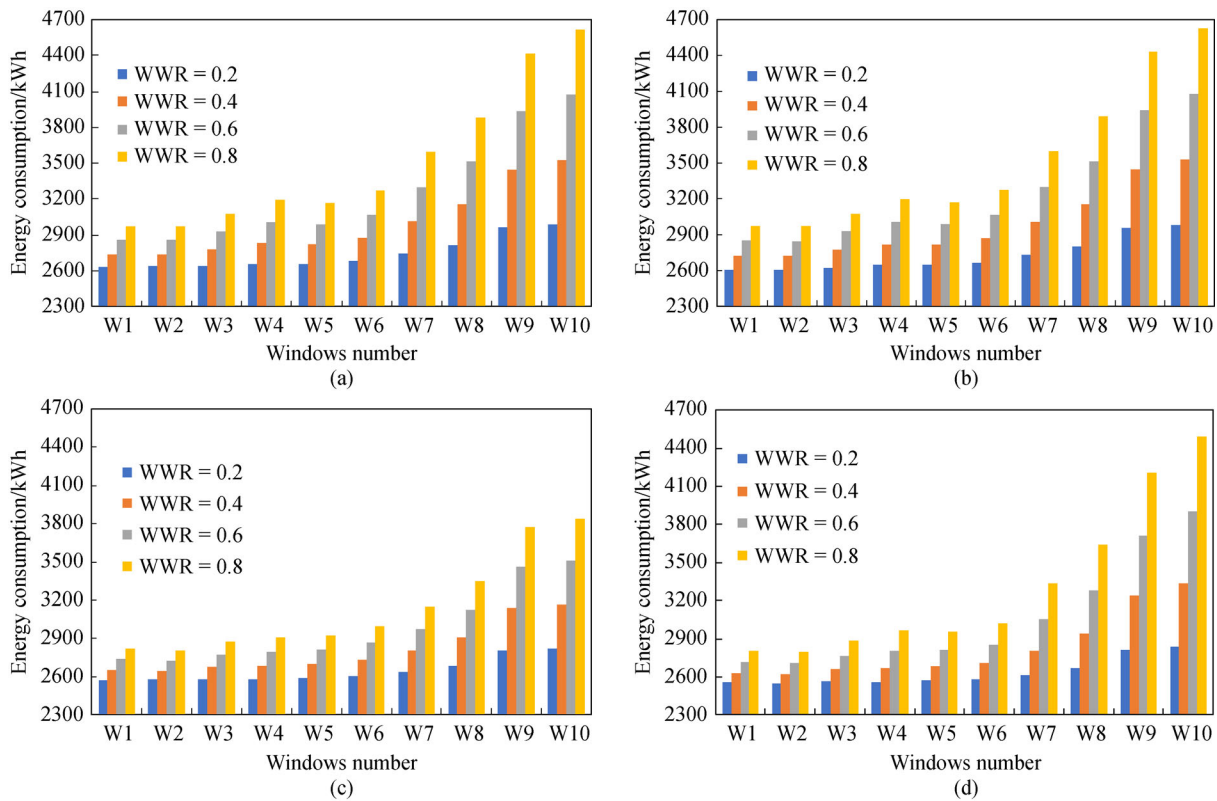


**Fig. 5** Energy consumption for the tested windows without the use of shading devices under various WWRs. (a) East facade; (b) west facade; (c) north facade; (d) south facade.

(W1–W3: with lower values of SHGC,  $U$ , and LT), medium-performance windows (W4–W6: with medium values of SHGC,  $U$ , and LT), and low-performance windows (W7–W10: with larger values of SHGC,  $U$ , and LT). In hot climates, the classification of the windows is dominated by the SHGC due to the high solar insolation. On the other hand, the  $U$ -value dominated the classification of windows in cold climates. Typically, the energy consumption of the room using W9 or W10 is considerably larger than that using W1–W3, for all facades. For example, at a WWR of 0.4, the room energy for W10 is larger than that of W1 by 29.38%, 28.96%, 26.82%, and 19.39% in the west, east, south, and north facades, respectively. This ratio increases as the WWR increases, e.g., in the south facade, the ratio of room energy using W10 to that using W1 increases from 14.25% at a WWR of 0.2 to 59.79% at a WWR of 0.8. This signifies the importance of the window specification on the energy consumption of the tested room.

The room energy consumption for all windows and facades increases as the WWR increases. The increase in the room energy with the WWR is caused by the increase in the cooling load of the room as the window area increases. This is indicated by an increase of the cooling electricity from 1820.6 to 2500.6 kWh (about 37.35%) as the WWR increases from 0.2 to 0.8, in the west facade using W6. Simultaneously, the heating electricity

decreases from 481.1 to 407.9 kWh (about 15.2%). It is worth noting that heating consumption is significantly lower than cooling consumption due to the cooling-dominated climate.

Importantly, the rate of increase in energy consumption with WWR depends strongly on the installed window type. This is supported by the fact that the changes in energy consumption with the WWR are limited when using W1 and W2 compared to those changes for W8–W10. This is demonstrated by the fact that in the south facade, the energy using W1 increases from 2552.5 to 2807.5 (255) kWh (10.0%) whereas the energy using W10 increases from 2839.6 to 4486.2 (1646.6) kWh (58.0%). Thus, the increase in room energy using W10 is 6.46 times that using W1 when the WWR increases from 0.2 to 0.8. Similar trends to these are noted on the other facades, as shown in Figs. 5(a)–5(d).

Figure 6 shows similar quantitative energy consumption for the room at a WWR of 0.4 for all windows. The high- and medium performance windows (W1–W6) achieve a lower energy consumption for windows in the south facade whereas the low-performance windows (W7–W10) attain a lower energy consumption for windows in the north facade. This may be explained by the variations of the heating and cooling consumptions in the different facades for a certain window type and a WWR. For example, the room using W6 with a WWR of 0.2 experiences an

increase in the annual cooling consumption from 1721.0 to 1828.0 (107) kWh and a decrease in the annual heating consumptions from 510.8 to 475.9 (34.9) kWh as the window facade changes from the north to the east direction. Similarly, the cooling electricity increases from 2139.4 to 2499.8 (360.4) kWh, and the heating electricity decreases from 490.9 to 398.4 (92.5) kWh, at a WWR of 0.8. Thus, as the room facade changes from north to east, the total heating and cooling consumptions of the room, using W6, increase from 2231.8 to 2303.9 (72.1) kWh at a WWR of 0.2 and from 2630 to 2898.2 (268.2) kWh at a WWR of 0.8 (Fig. 5).

The dividing condition to determine the best facade using unshaded windows is determined by the window facade parameter (WFP) defined by Eq. (9). The power of each parameter in the WFP points out the importance of the SHGC relative to  $U$  or the LT in a hot climate. Since in hot climate, the north facade can contribute more to building energy efficiency if it can dissipate heat more easily from indoor to outdoor. Therefore, windows with a high  $U$ -value and less radiative coating can be more beneficial. For the south glazing facades, more solar control ability is crucial for building energy efficiency. That means the window quality is mainly determined by the solar energy transmitted to the room more than the heat transfer by convection from outdoor to indoor.

$$\text{WFP} = \frac{LT^{0.1}}{\text{SHGC} \times U^{0.2}} \quad (9)$$

At a WWR of 0.4, the north facade requires the lowest energy if WFP is smaller than 2 (for low-performance windows), and the south facade requires the lowest energy when WFP is larger than 2 (for high-performance windows). In conclusion, the best building facade depends on the glazing quality, i.e., the north facade is the best for unshaded low-performance windows whereas the south facade is the best for high-performance windows. This may provide an answer to one of the contradictions in the

literature regarding the best facade orientation where either north or south facade is reported.

The effect of the window type on the energy consumption of the room in the various facades can be explained with the help of the window characteristics, particularly, the SHGC, and  $U$ . Figure 7(a) shows the total transmitted solar radiation that includes both beam and diffuse radiation through the different windows whereas Figs. 7(b) and 7(c) show the solar heat gain and the heat loss, respectively, of the tested windows in the four facades. The solar transmitted radiation (Fig. 7(a)) and the solar heat gain (Fig. 7(b)) are greater than the heat loss (Fig. 7(c)) by more than an order of magnitude. This makes the SHGC a more dominating factor than the  $U$ -value, which agrees with Ref. [26].

In general, the differences between transmitted radiation (Fig. 7(a)), solar heat gain (Fig. 7(b)), and heat loss (Fig. 7(c)) for high-and-medium performance windows are very limited compared to those for low-performance windows. This is denoted by the larger gaps between lines at a SHGC greater than 0.40 and a  $U$ -value greater than 1.6 W/(m<sup>2</sup>·K). The implication of this can be noted in Fig. 6 for the energy consumption of W1–W6. Additionally, the similar room energy required for the east and west facades (Fig. 6) can be explained by the similar total transmitted solar radiation, solar heat gain, and heat loss by the windows in those facades, as shown in Figs. 7(a)–7(c), respectively. However, the SHGC is a very important property for the window glass that affects the cooling and heating loads of the room, considerably. Moreover,  $U$  controls the amount of heat loss/gain from the window that influences the thermal load of the room. Although the north facade receives the lowest solar transmitted radiation, solar heat gain, and heat loss of all windows, the south facade requires the lowest heating load. Therefore, the lowest room energy is achieved using the low-performance windows for the room on the north facade, and the high-performance windows for the room on the south facade (Fig. 6).

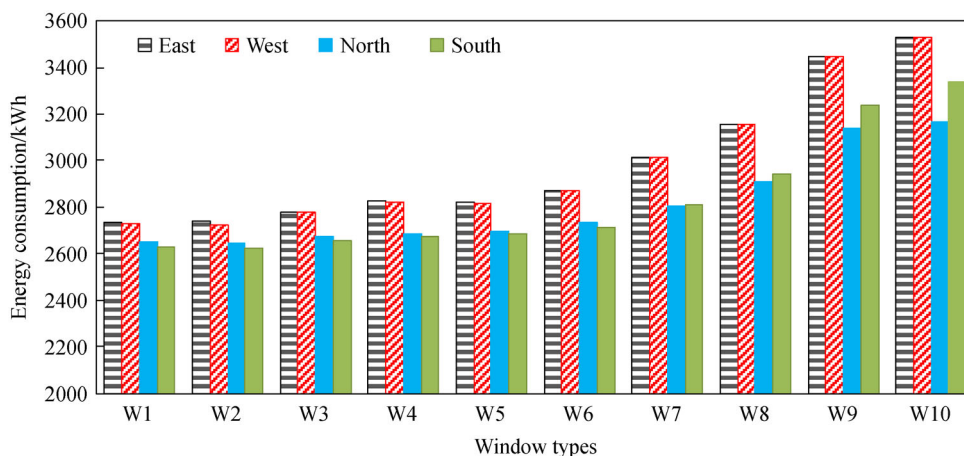
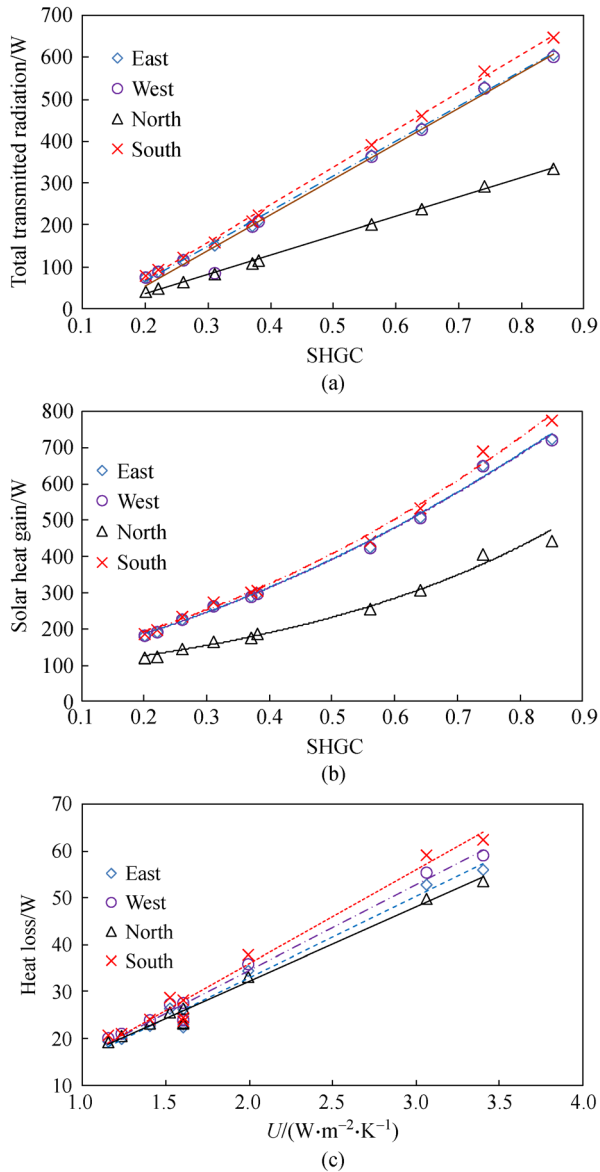


Fig. 6 Effect of facade orientation on energy consumption for the tested windows without the use of shading devices at a WWR of 0.40.



**Fig. 7** Effect of window properties on the window performance of the tested room.

(a) Total transmitted radiation; (b) solar heat gain; (c) heat loss.

In conclusion, the energy consumption of the room depends mainly on the window type and secondly on the WWR and facade orientation. Besides, buildings with windows on the north or south facade require the lowest energy consumption for low or high-performance windows, respectively. The magnitude of the variation of energy consumption with the WWR in the north facade is relatively smaller than that of the other facades (Fig. 5). Thus, high-performance windows on the north or south facade may use large a WWR without a significant scarfing in energy consumption.

### 5.2.2 Annual artificial lighting

As mentioned earlier, the energy consumption of artificial lighting is considerably lower than the total energy consumption (heating and cooling) by over an order of magnitude (0.04–0.095). The annual artificial lighting consumption for the unshaded tested windows at a WWR of 0.4 is listed in Table 4. The maximum lighting consumption is required by W2 and the minimum by W9 whereas W5 has an average energy consumption. The reason for this is that W2 has the lowest LT of 0.21, W9 has the maximum LT (1.0) and W5 has a LT of 0.50 as listed in Table 2. The lighting consumption of the windows varies from 2.63% to 8.44% for west and east facades, respectively. As expected, the artificial lighting consumption for a WWR of 0.2 is larger than that required for a WWR of 0.8 by average ratios of 1.49%, 2.91%, 4.31%, and 5.13% for west, south, north, and east facades.

### 5.3 Effect of design parameters on solar shaded fenestration

#### 5.3.1 Annual energy consumption

Table 5 lists the percentage effect of shading devices on the energy consumption of the tested room for the four facades, using the various window types. In general, the shading devices reduce the energy consumption of the room by 0.61% to 5.43% for a WWR of 0.2 and by 2.22%

**Table 4** Annual artificial lighting consumption (kWh) of the tested windows at a WWR of 0.4 on the unshaded four facades

Window	East	West	North	South
W1	204.5	194.6	200.6	199.4
W2	209.6	196.1	204.3	202.3
W3	200.0	193.1	197.2	196.5
W4	197.7	192.4	195.5	195.0
W5	197.8	192.4	195.6	195.1
W6	195.1	191.6	193.6	193.3
W7	194.3	191.4	193.0	192.8
W8	194.3	191.4	193.0	192.8
W9	192.9	191.0	192.0	192.0
W10	194.0	191.3	192.7	192.6

**Table 5** Percentage effect of full solar shading on energy consumption of the tested window types on each facade

Façade	East		West		North		South	
	WWR = 0.2	WWR = 0.8	WWR = 0.2	WWR = 0.8	WWR = 0.2	WWR = 0.8	WWR = 0.2	WWR = 0.8
W1–W3	0.66–1.16	4.05–5.86	1.03–1.39	4.60–6.34	0.61–0.67	2.22–3.34	0.60–0.91	3.22–5.35
W4–W6	1.51–1.75	7.37–8.86	1.70–1.94	7.82–9.30	0.86–1.01	4.24–4.68	1.17–1.36	7.44–9.53
W7–W10	2.68–4.79	13.13–20.88	2.82–5.00	13.43–21.04	1.57–2.83	7.69–12.14	2.13–5.43	16.53–32.39

to 32.39% for a WWR of 0.8 for all windows on the four facades. The lowest effect of shading devices is for those installed on the north facade (0.61–12.14), followed by the east (0.66–20.88), the west (1.03–21.04), and the south (0.60–32.39) facades. Table 5 indicates that W1–W3 can be used without the need to install any shading devices with a limited increase of the energy consumption that is lower than 1.39% for a WWR of 0.2 and 6.34% for a WWR of 0.8.

Based on the shading effectiveness, the high-performance windows (W1–W3) are found to be less sensitive to solar shading followed by medium (W4–W6), and high-performance windows (W7–W10) which are very sensitive to solar shading. The reason for that is attributed to the lower SHGC for W1–W3 (0.20–0.26) than W4–W6 (0.31–0.38) and W7–W10 (0.56–0.85). Thus, the shading devices are essential for low-performance windows (high SHGC) than for high-performance windows (low SHGC) that may work without the solar shading devices with limited scarifies in energy, particularly for a low WWR.

The necessity of solar shading installation can be correlated with the window SHGC and WWR. Based on an annual allowance of 5% or 120 kWh (whatever less) increase in the room energy over the full shading condition, the window SHGC can be identified for each facade and WWR. Based on the stated conditions, the obtained SHGC is correlated with the WWR for the north (Eq. (10)) and other facades (Eq. (11)). Both equations have correlation coefficients greater than 0.9976. Thus, if the SHGC of the window is equal to or lower than the values obtained by Eq. (10) or (11), solar shading is not essential.

$$\text{For north facade, } \text{SHGC} \leq 0.3175 \text{WWR}^{-0.614}. \quad (10)$$

For east, west, and south facades,

$$\text{SHGC} \leq 0.161 \text{WWR}^{-0.945}. \quad (11)$$

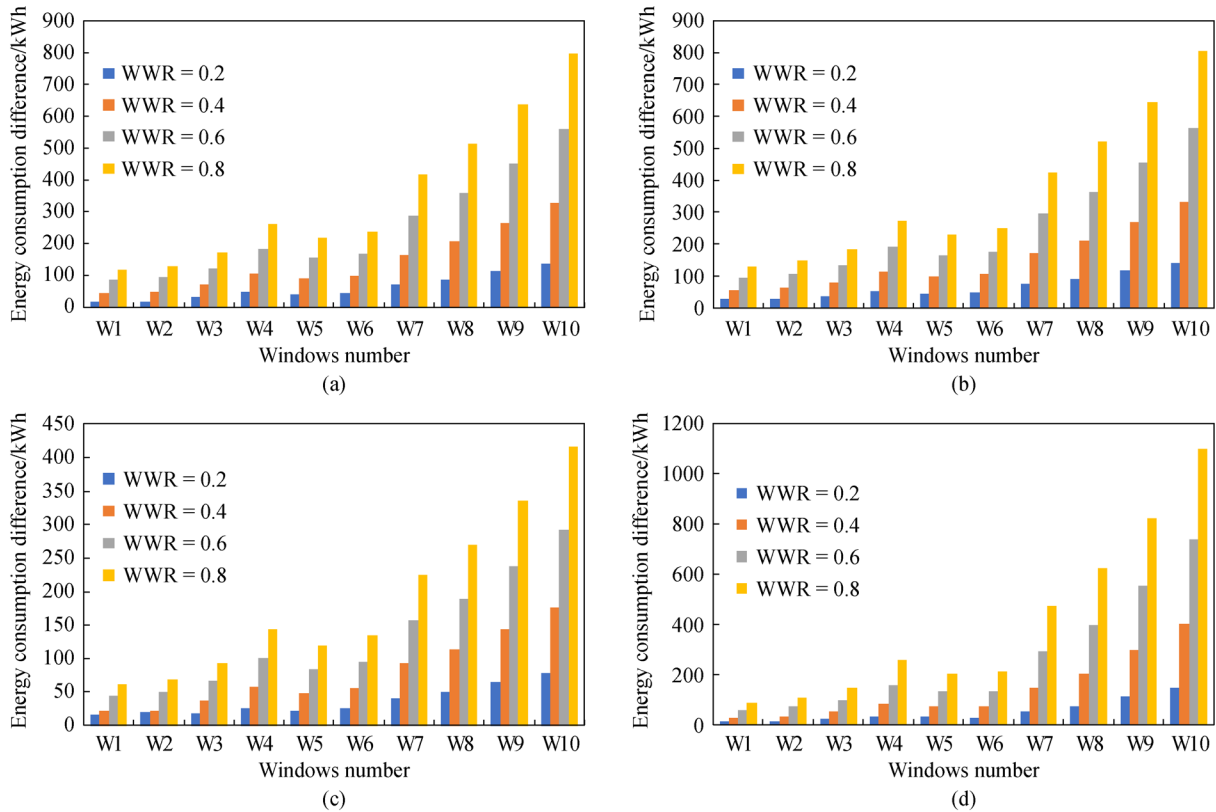
The saved energy due to the installation of full overhang and side-fin shading devices on the ten tested windows for a WWR of 0.2, 0.4, 0.6, and 0.8 is presented in Figs. 8(a)–8(d) for each facade orientation. The effect of solar shading depends strongly on the installed window type, i.e., SHGC. It is noted that the largest saving due to shading devices is on the south facade using W10 (the lowest-performance window). This is due to the various

specification of the windows, particularly the SHGC.

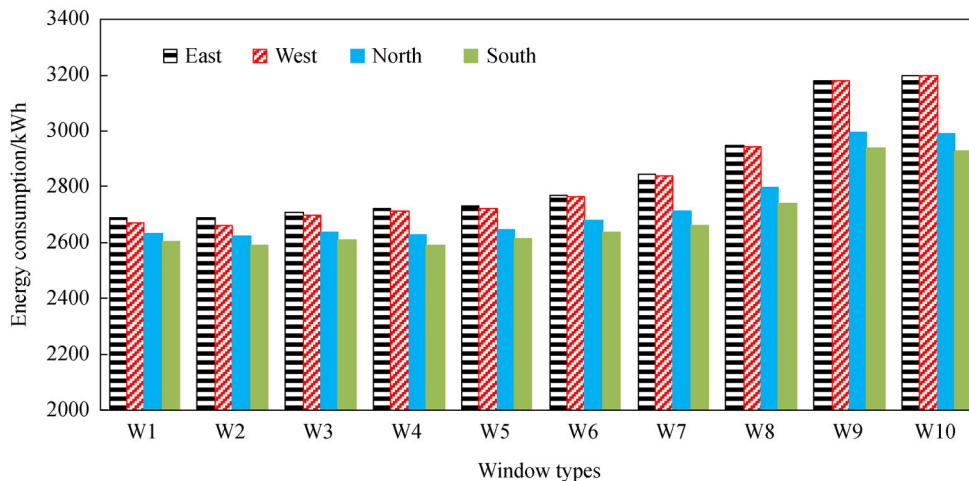
Figure 8 shows that the north facade is the least affected by solar shading for all window types. This is demonstrated by the magnitude and percentage of the effect of shading devices on the room energy using W10 with a WWR of 0.4 that provides 405.2 kWh (12.1%) for the south, 331.6 kWh (9.4%) for the west, 326.8 kWh (9.3%) for the east, and 176.3 kWh (5.6%) for north facades. However, the energy-saving due to shading devices using W1 for the same WWR of 0.4 is 56 kWh (2.05%) for the west, 44.7 kWh (1.63%) for the east, 29.2 kWh (1.11%) for the south, and 21.4 kWh (0.81%) for north facades. Notably, the shading effect increases as the WWR increases, for any of the facade orientations or window types. For example, as the WWR increases from 0.2 to 0.8, the shading effect increases from 26.5 to 130.9 kWh (1.02%–4.40%) when using W1 on the west facade and from 146.4 to 1097.6 kWh (5.15%–24.47%) when using W10 on the south facade.

Figure 9 shows the annual energy consumption of the room using the various tested windows with full-solar shading at a WWR of 0.4 for the four main facade orientations. The rooms with windows on the south facade attain the lowest energy consumption for either low- or high-performance windows. Constantly, the north facade has a larger energy consumption than the south one for the solar shaded windows. Therefore, the south facade is the best for all shaded windows and for high-performance unshaded windows whereas the north facade attains a lower energy for low-performance unshaded windows. This may resolve the contradiction of the best facade orientation in the literature between the north (Refs. [15,16]) and the south (Ref. [19]) facades.

In conclusion, the effect of the shading device on the room energy differs from one window to another as W10 is the most influenced by the shading devices and W1–W3 are the least affected by the shading devices. Therefore, the room using W1 or W2 may not install an overhang or side-fins shading device without prejudicing energy consumption, particularly when the room is on the north or south facade using a reasonable WWR. This is supported by relatively limited annual energy savings due to the shading devices when using W1 and W2, of about 20.2–68.9, 17.4–106.6, 17.96–129.5, and 29.7–150.0 kWh on the north, south, east, and west facades, respectively, for WWR of 0.2–0.8. Such windows (W1 and W2) may be used to retrofit windows in existing residential houses to reduce



**Fig. 8** Effect of full shading devices on the energy consumption of the various windows under different facade orientations and WWRs. (a) East facade; (b) west facade; (c) north facade; (d) south facade.



**Fig. 9** Effect of facade orientation on the energy consumption for the full-shaded tested windows at a WWR of 0.40.

their energy consumption without the need to install shading devices.

The above discussion considers the effect of full solar shading of overhangs and side-fins. However, the nine shading conditions include the possible combinations of full (half of the window height), half (a quarter of the window height), and no overhang projection combining

with full (half the window width), half (a quarter of the window width), and no side-fins projection. The effect of partial solar shading is discussed in the following paragraphs.

Table 6 lists the annual energy saving due to full overhang, side-fins, or combined solar shading, in kWh and percentage, using W1 or W10 for a WWR of 0.2 and

0.8, when the room facade is on the four main orientations. Again, the effect of shading devices on the room energy is more pronounced for the low-performance window (W10) than the high-performance window (W1). Generally, the side-fins are more effective on the north and south facades whereas the overhang performs better on the east and west facades. In addition, the overhangs have a negative effect on energy-saving using the high-performance window (W1) at a low WWR (0.2) of the north facade. Therefore, there is no need to install overhangs in the north facades or when using high-performance windows, particularly for a low WWR. On the other hand, the maximum effect of shading is on the south facade using low-performance windows (W10), particularly at a high WWR of 0.8, as the combined effect of shading devices under these conditions on the south facade is 2.64 times that in the north facade (Table 6).

The effect of the nine shading conditions on the annual room energy due to the increase of the WWR from 0.2 to 0.8 using either W1 or W10 is listed in Table 7, on the four facades. Table 7 indicates that the lowest annual consequence (181.3 kWh) due to the increase of the WWR from 0.2 to 0.8 takes place for the room using W1 on the south facade under the full overhang and side-fin shading condition. Moreover, the lowest annual consequence (251.6 kWh) without shading devices occurs on the north facade using W1. Conversely, the largest consequence (1646.6 kWh) is for the room using W10 on the south facade, without shading devices. Thus, the monthly increase in energy consumption due to the increase of WWR from 0.2 to 0.8 varies from 15.13 to 137.21 kWh (over nine times) due to window type and shading

conditions. As the WWR increases from 0.2 to 0.8, the shading effect increases from about 26% (for W1 on the north facade) to about 137% (for W10 on the south facade). The ratio of the room energy consumption increase using W10 to that using W1 ranges from 3.43 to 3.88 (under full shading conditions) to 4.07–6.46 (under no shading conditions). Therefore, the effect of window characteristics is much more significant than that of shading devices, particularly for a high WWR.

### 5.3.2 Annual artificial lighting

The annual artificial lighting consumption varies with the facade orientation, WWR, window type, and shading devices. As expected, the artificial lighting consumption for WWR of 0.2 is larger than that required for WWR of 0.8. Table 8 lists the percentage effect of shading devices on the artificial lighting energy for the four facades. The effect of shading devices on the cases of WWR of 0.8 is more significant than on the cases of WWR of 0.2. Generally, the shading devices affect the lighting energy by 0.28% to 8.12%. The lowest effect of the shading devices on the lighting energy is on the west (0.28%–1.84%) facade followed by south (0.73%–3.96%), north (0.77%–6.52%), and east (1.08%–8.12%) facades.

The effect of shading devices on the artificial lighting energy of the room using W1–W3 is more influential than those using W4–W6 and W7–W10. This is contradicting the effect of shading devices on the energy consumption of the room using the various windows, i.e., the windows that are less affected by the shading devices on the energy consumption are the more affected by the shading devices

**Table 6** Energy saving in kWh and percentage (%) of windows 1 and 10 at a WWR of 0.2 and 0.8 under different shading conditions

Shading condition	WWR = 0.2		WWR = 0.8	
	W1	W10	W1	W10
East facade/kWh (%)				
Full side-fin	8.40 (0.32)	45.40 (1.59)	35.75 (1.25)	298.05 (7.80)
Full overhang	8.80 (0.34)	91.40 (3.20)	79.85 (2.80)	499.45 (13.07)
Combined (full)	17.30 (0.66)	136.80 (4.79)	115.60 (4.05)	797.50 (20.88)
West facade/kWh (%)				
Full side-fin	9.28 (0.36)	46.85 (1.65)	43.55 (1.53)	304.90 (7.98)
Full overhang	17.20 (0.67)	95.25 (3.35)	87.33 (3.07)	499.32 (13.06)
Combined (full)	26.48 (1.03)	142.10 (5.00)	130.88 (4.60)	804.22 (21.04)
North facade/kWh (%)				
Full side-fin	11.3 (0.44)	58.3 (2.13)	44.8 (1.62)	284.7 (8.31)
Full overhang	-2.25 (-0.09)	19.4 (0.71)	16.5 (0.60)	131.3 (3.83)
Combined (full)	9.0 (0.35)	77.7 (2.83)	61.3 (2.22)	415.9 (12.14)
South facade/kWh (%)				
Full side-fin	7.9 (0.31)	59.6 (2.21)	39.9 (1.47)	481.5 (14.21)
Full overhang	5.9 (0.23)	86.8 (3.22)	47.7 (1.75)	616.1 (18.18)
Combined (full)	13.8 (0.55)	146.4 (5.43)	87.6 (3.22)	1097.6 (32.39)

**Table 7** Increase in energy consumption (kWh) due to the increase of WWR from 0.2 to 0.8 of W1 or W10 under different shading conditions

Overhang condition	Side-fin condition	East		West		North		South	
		W1	W10	W1	W10	W1	W10	W1	W10
Full	Full	248.5	965.3	267.7	978.2	199.4	684.5	181.3	695.3
Half	Full	285.5	1143.3	301.7	1153.0	209.6	732.1	195.2	873.3
Zero	Full	317.1	1358.4	337.2	1368.3	217.8	799.4	220.3	1184.9
Full	Half	261.8	1079.5	285.9	1095.5	214.5	782.9	193.6	852.6
Half	Half	300.6	1262.4	320.0	1274.3	224.7	825.9	208.5	1051.9
Zero	Half	333.5	1485.2	356.0	1497.8	233.3	893.2	235.7	1385.2
Full	Zero	273.4	1203.0	301.3	1222.3	232.7	913.9	210.6	1077.6
Half	Zero	313.3	1394.6	336.0	1409.6	243.6	959.0	227.4	1302.0
Zero	Zero	346.9	1626.0	372.1	1640.3	251.6	1022.8	255.0	1646.6

**Table 8** Percentage effect of full solar shading on the artificial lighting consumption for the tested window types on each facade

Facade	East		West		North		South	
	WWR = 0.2	WWR = 0.8	WWR = 0.2	WWR = 0.8	WWR = 0.2	WWR = 0.8	WWR = 0.2	WWR = 0.8
W1–W3	2.36–4.78	4.53–8.12	0.54–0.75	1.25–1.84	1.64–4.36	3.51–6.52	1.32–2.26	3.05–3.96
W4–W6	1.44–1.87	2.92–3.79	0.38–0.48	0.84–1.06	1.03–1.32	2.23–2.94	0.94–1.15	1.94–2.59
W7–W10	1.08–1.35	2.03–2.65	0.28–0.36	0.57–0.75	0.77–0.96	1.51–2.01	0.73–0.89	1.30–1.79

on the lighting energy. The reason for that is the lower LT property for W1–W3 (0.21–0.4) than W4–W6 (0.5–0.76) or W7–W10 (0.76–1.0).

#### 5.4 Cost analysis

The economic analysis supports the selection of a cost-effective window type that saves more energy than others or installing a solar shading of overhangs or side-fins to the exterior sides of the windows. Thus, the economic benefits are attained by improving the window system either by replacing low-performance windows with a more efficient one or installing an appropriate solar shading device. As a result, this would encourage householders to either retrofit their existing windows or choose an efficient window system for their new buildings. The NPV for all windows or shading devices is calculated for a 30-years financial plan as discussed in Section 4. Positive NPV indicates rewarding cases and negative NPV represents ineffective cases.

##### 5.4.1 Cost analysis for windows without solar shading

In this section, a detailed economic analysis is presented for windows without the use of overhangs or side fins as external solar shading devices. Both NPV and the SPP are calculated based on the difference between the price of each window and that of window 10. Thus, both the NPV and SPP reflect the potential of replacing W10 with other high-performance windows. The NPV and SPP for W1–W9 are listed in Table 9 (for a WWR of 40% oriented on the east, west, north, and south facades) and in Table 10 for

the west facade at a WWR of 20%, 40%, 60%, and 80%. Based on the results in Tables 9 and 10, W1 and W2 are found to have the largest NPV while W1 and W4 have the lowest SPP compared to other studied windows. Thus, W1 represents the best economical choice regarding both the NPV and the SPP.

Table 9 indicates that replacing W10 with either of the studied windows has a substantial positive economic value for all facades with different degrees. For instance, W8 and W9 have the same cost as W10, thus, the SPP is zero for either of them whereas the NPV is considerable particularly for W8. A NPV of up to 2277.1 USD is achieved due to replacing W10 with W1 of a WWR 40% on the west facade. The largest NPV and lowest SPP are achieved, by all windows, on the west/east facades followed by the south facade whereas the north facade has the lowest NPV and the largest SPP. An SPP as low as 1.46/1.48 years is achieved by W1 with a WWR of 40% on the west/east facade.

Table 10 shows that the NPV increases as the WWR increases from 20% to 80%. Except for W9, all other windows achieve a considerable NPV, indicating the feasibility of replacing the present low-performance window. Again, W8 achieves about half the NPV of W1 without any additional cost. Apart from the SPP of zero for W8 and W9, the SPP of windows on the west facade ranges from 1.46 years for W1 at a WWR of 40% to 7.30 years for W7 at a WWR of 80%.

##### 5.4.2 Cost analysis for windows with solar shading

This section examines the value of adding external solar



**Table 9** Economical evaluation of windows on various facades at a WWR of 40% without shading

Window	NPV/USD				SPP <sub>wf/a</sub>			
	East	West	North	South	East	West	North	South
W1	2249.2	2277.1	1408.6	1987.9	1.48	1.46	2.27	1.66
W2	2153.2	2195.0	1342.6	1920.1	2.38	2.34	3.60	2.64
W3	2023.3	2040.1	1248.6	1815.3	2.52	2.50	3.83	2.77
W4	1969.0	1983.3	1308.2	1864.8	1.67	1.66	2.43	1.76
W5	1862.9	1873.8	1146.6	1698.0	3.09	3.08	4.65	3.35
W6	1815.5	1824.1	1136.1	1723.4	2.09	2.08	3.17	2.19
W7	1319.8	1327.9	855.8	1362.9	3.65	3.63	5.20	3.55
W8	1122.3	1125.9	781.7	1188.1	0	0	0	0
W9	248.5	238.3	75.7	303.5	0	0	0	0

**Table 10** Economical evaluation of windows at various WWR on the west facade without shading

Window	NPV/USD				SPP <sub>wf/a</sub>			
	20%	40%	60%	80%	20%	40%	60%	80%
W1	1082.5	2277.1	3273.6	4404.8	1.53	1.46	2.85	2.83
W2	1039.4	2195.0	3012.8	4052.4	2.46	2.34	4.58	4.55
W3	972.3	2040.1	2772.4	3728.6	2.61	2.50	4.90	4.86
W4	957.0	1983.3	2799.3	3734.5	1.72	1.66	3.27	3.27
W5	895.6	1873.8	2457.1	3299.3	3.20	3.08	6.04	6.01
W6	875.0	1824.1	2535.6	3403.3	2.16	2.08	4.08	4.05
W7	645.0	1327.9	1647.3	2169.1	3.72	3.63	7.24	7.30
W8	548.0	1125.9	1694.9	2235.5	0	0	0	0
W9	95.3	238.3	411	600.9	0	0	0	0

shading of both overhang (with a projection equals half the window height) and side fins (half the window width) to the exterior side of each of the considered windows. This cost analysis indicates the feasibility of installing shading devices for each of the studied windows. Again, the NPV of external solar shading is based on a 30-years financial plan.

Table 11 indicates that solar shading devices are more feasible on the west, east, and south facades than on the north facade. The best-performance windows (W1–W3) do not need shading devices to enhance their performance. Such windows attain negative NPV and exceptionally long SPP for all facades, demonstrating that installing shading devices is not a feasible solution. On the other hand, low-performance windows (W7–W10) attain a positive NPV and a reasonable SPP, for all facade orientations. W10 is the most suitable window for shading installation as it achieves the largest NPV and the shortest SPP. This is due to its lowest performance compared to the other considered windows. The discussed results about the shading effect implicate that replacing existing low-performance windows with high-performance ones is a feasible retrofitting solution that is easy to implement without the need to install fixed or attached shading devices.

Table 12 lists the NPV and SPP for the windows on the west facade with WWRs of 20%–80% due to installing shading devices for the considered windows. In general, the NPV increases and the SPP decreases as the WWR increases, for all windows. Again, the high-performance windows attained a negative NPV and a long SPP whereas the low-performance windows achieve a reasonable NPV and SPP for all WWRs on the west facades due to installing the solar shading overhang and side-fin.

### 5.5 Concluding discussion of the fenestration characteristics

The cost analysis manifests that the high-performance window (W1) affords the cost-effective window among the tested ones. Therefore, a comparison between the annual energy consumption of the tested room on the four facades using W1 or the low-performance window (W10) is shown in Fig. 10(a) for the case without solar shading and in Fig. 10(b) with full solar shading. The annual energy consumption is compared for a WWR of 0.2, 0.4, 0.6, and 0.8. Under all conditions, the room energy using W1 is considerably lower than that using W10. Additionally, the energy consumption using W1 on the south orientation is

**Table 11** Economical evaluation of solar shading of the windows at a WWR of 40% on various facades

Window	NPV/USD				SPP <sub>ws/a</sub>			
	East	West	North	South	East	West	North	South
W1	-124.1	-89.9	-194.6	-170.9	46.06	36.75	96.10	70.41
W2	-117.8	-67.4	-194.7	-155.2	44.00	32.45	96.34	59.80
W3	-47.2	-22.5	-148.6	-102.2	29.36	26.30	56.22	39.63
W4	60.6	81.9	-84.3	-6.0	19.46	18.25	35.59	24.59
W5	13.5	35.8	-113.8	-42.0	22.83	21.10	42.78	28.66
W6	41.2	56.4	-92.1	-42.9	20.72	19.73	37.24	28.78
W7	242.3	258.3	22.8	184.8	12.42	12.03	22.07	14.02
W8	362.4	380.5	82.3	354.5	10.02	9.73	18.23	10.15
W9	545.6	560.2	178.1	646.0	7.74	7.60	14.24	6.88
W10	729.8	744.0	274.0	649.0	6.30	6.21	11.68	6.86

**Table 12** Economical evaluation of solar shading of the windows on the west facade for various WWRs

Window	NPV/USD				SPP <sub>ws/a</sub>			
	20%	40%	60%	80%	20%	40%	60%	80%
W1	-54.3	-89.9	-113.7	-135.8	40.29	36.75	33.59	32.25
W2	-44.7	-67.4	-73.6	-78.0	35.97	32.45	29.45	28.14
W3	-25.2	-22.5	-0.8	24.3	29.57	26.30	24.07	22.97
W4	17.6	81.9	178.1	291.4	21.24	18.25	16.60	15.52
W5	-0.4	35.8	96.3	164.7	24.09	21.10	19.34	18.34
W6	7.4	56.4	130.6	217.5	22.77	19.73	18.09	17.05
W7	92.2	258.3	492.5	756.4	14.25	12.03	10.75	9.91
W8	144.5	380.5	700.5	1050.9	11.58	9.73	8.71	8.07
W9	224.5	560.2	983.2	1421.4	9.00	7.60	6.93	6.54
W10	295.5	744.0	1309.0	1901.7	7.51	6.21	5.61	5.25

lower than those on the other facades in both cases with and without solar shading devices, particularly for a low WWR. On the other hand, the room using W10 shows a better performance on the north facade in the case without shading and on the south facade with full shading devices, as can be seen in Fig. 10(b). This is due to the large effect of shading devices using W10 on the south facade, as seen in Fig. 8(d). Therefore, the room on the south facade requires the lowest energy when using W1 with or without shading and using W10 with a full shading device. In conclusion, the shading effect on rooms using W1 is considerably lower than those using W10 (compare Figs. 10(a) and 10(b)).

Using the data presented in Fig. 10, the energy difference (kWh) and the energy difference per unit window area (kWh/m<sup>2</sup>) for the building using W10 and W1 are listed in Table 13, for a WWR of 0.2–0.8. The energy difference between W10 and W1 is listed for three cases (a) without solar shading for both windows, (b) with solar shading for both windows, and (c) with solar shading

for W10 and without shading for W1. All cases show that the building using the high-performance window (W1) consumes lower energy than that using a low-performance window (W10) even in case (c) where W1 is without shading and W10 with full solar shading.

Table 13 indicates that the energy difference per unit window area can be presented by a mean value with a reasonable standard deviation (STD), except for the south facade when both windows are not shaded. The mean energy difference/unit window area for the east and west facades are close to each other. A normal size residential building of 13 m × 22 m × 4 m with three floors may have windows of about 55 m<sup>2</sup> (WWR 0.35) on the facade side and about 60 m<sup>2</sup> on the other three sides of the building. Thus, about 115 m<sup>2</sup> of glazing is distributed on the four orientations. Replacing the existing window (W10) with the high-performance window (W1) results in an energy-saving of about 12.7 MWh for case (a), and 7.57 MWh for case (b). In addition to the energy-saving, the corresponding reduction in CO<sub>2</sub> emission is about 11.05 tons for case

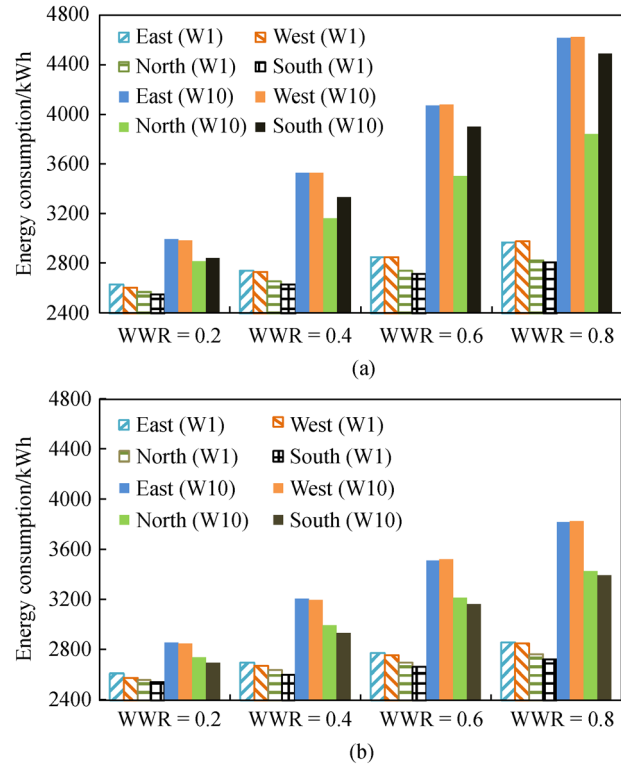


**Fig. 10** Annual energy consumption using W1 and W10 for different facades and WWRs. (a) Without solar shading; (b) with shading devices.

**Table 13** Energy saving due to replacing a low-performance window (W10) with a high-performance window (W1)

WWR/ Façade	Energy saving/kWh				Energy saving/unit area of window/(kWh·m <sup>-2</sup> )					
	0.2	0.4	0.6	0.8	0.2	0.4	0.6	0.8	Mean	STD (%)
(a) Without shading for W1 and W10										
East	366.3	791.9	1220.6	1645.5	114.5	123.7	127.1	128.6	123.5	6.3 (5.1)
West	382.1	801.1	1227.7	1650.3	119.4	125.2	127.9	128.9	125.3	4.3 (3.4)
North	247.2	514.1	770.6	1018.4	77.3	80.3	80.3	79.6	79.4	1.4 (1.8)
South	287.2	705.6	1184.0	1678.7	89.7	110.2	123.3	131.2	113.6	18.1(15.9)
(b) With full shading for W1 and W10										
East	246.8	509.7	745.5	963.6	77.1	79.6	77.7	75.3	77.4	1.8 (2.3)
West	266.4	525.5	757.6	976.9	83.3	82.1	78.9	76.3	80.2	3.1 (3.9)
North	178.6	359.3	522.8	663.7	55.8	56.1	54.5	51.9	54.6	1.9 (3.6)
South	154.6	329.7	502.2	668.7	48.3	51.5	52.3	52.2	51.1	1.9 (3.6)
(c) Without shading for W1 and full shading of W10										
East	229.5	465.1	660.9	848.0	71.7	72.7	68.8	66.2	69.9	2.9 (4.2)
West	240.0	469.5	663.3	846.0	75.0	73.4	69.1	66.1	70.9	4.0 (5.7)
North	169.5	337.9	477.9	602.4	53.0	52.8	49.8	47.1	50.7	2.8 (5.5)
South	140.8	300.4	443.2	581.1	44.0	46.9	46.2	45.4	45.6	1.3 (2.7)

(a), and 6.43 tons for case (b). The annual saved energy in cases (a) and (b) results in a reduction of the electricity bill of about 1600 and 954 USD, respectively.

## 6 Summary and conclusions

The main contradictions about the best fenestration

characteristics (glazing quality, window orientation, and cost-effectiveness) that existed in the literature are explained by thoroughly investigating the effect of building fenestration characteristics on the energy consumption of residential buildings in a hot climate. The considered characteristics include facade orientation, WWR, glazing properties, and solar shading. A cubic room with a 4 m side is simulated using building simulation (EnergyPlus) and jEPlus programs. Energy performance analysis is conducted using the optimization technique followed by a parametric study. In addition, a cost analysis study, for windows with or without solar shading, identifies the cost-effective cases. The obtained results encourage householders to either retrofit their existing windows or choose an efficient window system for their newly constructed buildings. Based on the reported results the following conclusions may be drawn:

The window glazing properties control the effect of the other fenestration characteristics. The south facade is the best for all solar-shaded windows and unshaded high-performance windows when the parameter  $LT^{0.1}/(SHGC \times U^{0.2})$  is greater than 2.0 whereas the north facade is the best for unshaded low-performance windows when  $LT^{0.1}/(SHGC \times U^{0.2})$  is less than 2. Besides, the window glazing properties determine the need for solar shading as the solar shading reduces the energy consumption by about 32.39% for low-performance windows and only 6.35% for high-performance windows, which depends mainly on the SHGC. Moreover, glazing properties regulate the effect of the window to wall ratio. For example, as the WWR increases from 0.2 to 0.8, the building energy consumption using the low-performance window is 6.46 times of that using the high-performance window. Furthermore, at a WWR of 0.4, the room energy for the lowest-performance window is larger than that of the highest-performance window by 29.38%, 28.96%, 26.82%, and 19.39% in the west, east, south, and north facades, respectively.

The need for solar shading is correlated with the SHGC and WWR. The solar shading on the north facade should be carefully selected as the overhangs have a negative effect on the room energy using high-performance windows of small size. Nevertheless, the side-fins are more effective on the north facade whereas the overhang performs better on the other facades.

The economic analysis reveals that the best-performance window (double glazing air-filled low-e sun-guard double sliver 6 mm-12 mm-6 mm) without solar shading is the cost-effective choice as it has the largest NPV and the shortest SPP. Additionally, solar shading is economically feasible for low-performance windows, but not for high-performance windows.

The window glazing quality is the most influential design parameter on the energy consumption, followed by the WWR, facade orientation, and shading condition. The effect of the WWR and solar shading on the lighting energy is opposite to that on the energy consumption.

The high-performance window is less sensitive to the increase in the window size as less than a 10% increase in energy consumption is experienced as the WWR increases from 0.2 to 0.8.

Although the study focused on a residential building, the methodology and the conclusion may be applied to most of the other building types as the effect of lighting energy is limited, particularly in hot climate countries.

**Acknowledgements** This work was funded by the Public Authority for Applied Education and Training (PAAET) under project number TS-08-14.

## Notations

$B_w$	Window luminance/( $\text{cd} \cdot \text{m}^{-2}$ )
CF	Cash flow/USD
$E_{w10}$	Annual electrical energy consumed by the room using W10/kWh
$E_{wi}$	Annual electrical energy consumed by the room using window W1–W9/kWh
GC	Glazing cost/USD
GCD	Difference between window GC and window 10 GC/USD
$i_L$	Reference point index
$i_s$	Window shade index
$I_{set}$	Illuminance setpoint/lux
$n$	Number of years
$NPV_{ws}$	Net present value for windows with solar shading/USD
$NPV_{wt}$	Net present value for windows without solar shading/USD
PC	Production cost of electrical energy/( $0.126 \text{ USD} \cdot \text{kWh}^{-1}$ )
PV	Present value/USD
$r$	Discount rate/1.5%
$S_w$	Window background luminance/( $\text{cd} \cdot \text{m}^{-2}$ )
SSC	Solar shading cost/( $\text{USD} \cdot \text{m}^{-2}$ )
$SPP_{ws}$	Simple payback period with solar shading/a
$SPP_{wt}$	Simple payback period without solar shading/a
$U$	Overall heat transfer coefficient of windows/( $\text{W} \cdot \text{m}^{-2} \cdot \text{K}^{-1}$ )
WFP	Window facade parameter
$\rho_b$	Area-weighted average reflectance of zone interior surfaces
$\omega$	Solid angle subtended by the window/steradians
$\Omega$	Modified solid angle subtended by the window/steradians

## Abbreviations

ACH	Air change
EUI	Energy use intensity
GA	Genetic algorithm
GCC	Gulf council countries
IDF	Input definition file
LT	Light transmission
NZEB	Net zero energy building
PMV	Predicted mean vote thermal occupant's comfort index
SHGC	Solar heat gain coefficient

STD	Standard deviation
TMY	Typical meteorological year
$W_{\#}$	Window number
WWR	Window-to-wall ratio

## References

- IEA. Tracking Building 2020. 2020–7, available at website of IEA
- Nejat P, Jomehzadeh F, Taheri M M, et al. A global review of energy consumption, CO<sub>2</sub> emissions and policy in the residential sector (with an overview of the top ten CO<sub>2</sub> emitting countries). *Renewable & Sustainable Energy Reviews*, 2015, 43: 843–862
- Ihm P, Krarti M. Design optimization of energy efficient residential buildings in Tunisia. *Building and Environment*, 2012, 58: 81–90
- AlAjmi A, Abou-Ziyan H, Ghoneim A. Achieving annual and monthly net-zero energy of existing building in hot climate. *Applied Energy*, 2016, 165: 511–521
- Belussi L, Barozzi B, Bellazzi A, et al. A review of performance of zero energy buildings and energy efficiency solutions. *Journal of Building Engineering*, 2019, 25: 100772
- Lu Y, Wang S, Shan K. Design optimization and optimal control of grid-connected and standalone nearly/net zero energy buildings. *Applied Energy*, 2015, 155: 463–477
- Alaidroos A, Krarti M. Optimal design of residential building envelope systems in the Kingdom of Saudi Arabia. *Energy and Building*, 2015, 86: 104–117
- Dias Barkokebas R, Chen Y, Yu H, et al. Achieving housing energy-efficiency requirements: methodologies and impacts on housing construction cost and energy performance. *Journal of Building Engineering*, 2019, 26: 100874
- Boafo F E, Ahn J G, Kim S M, et al. Fenestration refurbishment of an educational building: experimental and numerical evaluation of daylight, thermal and building energy performance. *Journal of Building Engineering*, 2019, 25: 100803
- Abediniangerabi B, Shahandashti S M, Makhmalbaf A. A data-driven framework for energy-conscious design of building facade systems. *Journal of Building Engineering*, 2020, 29: 101172
- Gao Y, He F, Meng X, et al. Thermal behavior analysis of hollow bricks filled with phase-change material (PCM). *Journal of Building Engineering*, 2020, 31: 101447
- Bhamare D K, Rathod M K, Banerjee J. Numerical model for evaluating thermal performance of residential building roof integrated with inclined phase change material (PCM) layer. *Journal of Building Engineering*, 2020, 28: 101018
- Strith U, Tyagi V V, Stropnik R, et al. Integration of passive PCM technologies for net-zero energy buildings. *Sustainable Cities and Society*, 2018, 41: 286–295
- Sun Y, Wilson R, Wu Y. A review of Transparent Insulation Material (TIM) for building energy saving and daylight comfort. *Applied Energy*, 2018, 226: 713–729
- Feng G, Chi D, Xu X, et al. Study on the influence of window-wall ratio on the energy consumption of nearly zero energy buildings. *Procedia Engineering*, 2017, 205: 730–737
- Persson M L, Roos A, Wall M. Influence of window size on the energy balance of low energy houses. *Energy and Building*, 2006, 38(3): 181–188
- Manz H, Menti U P. Energy performance of glazings in European climates. *Renewable Energy*, 2012, 37(1): 226–232
- Potrč Obrecht T, Premrov M, Žegarac Leskovar V. Influence of the orientation on the optimal glazing size for passive houses in different European climates (for non-cardinal directions). *Solar Energy*, 2019, 189: 15–25
- Dutta A, Samanta A, Neogi S. Influence of orientation and the impact of external window shading on building thermal performance in tropical climate. *Energy and Building*, 2017, 139: 680–689
- Leskovar V Ž, Premrov M. An approach in architectural design of energy-efficient timber buildings with a focus on the optimal glazing size in the south-oriented facade. *Energy and Building*, 2011, 43(12): 3410–3418
- Leskovar V Ž, Premrov M. Design approach for the optimal model of an energy-efficient timber building with enlarged glazing surface on the south facade. *Journal of Asian Architecture and Building Engineering*, 2012, 11(1): 71–78
- Leskovar V Ž, Premrov M. Influence of glazing size on energy efficiency of timber-frame buildings. *Construction & Building Materials*, 2012, 30: 92–99
- Ayse A, Muhsin K. Influence of window parameters on the thermal performance of office rooms in different climate zones of Turkey. *International Journal of Renewable Energy Research*, 2019, 9: 226–243
- Gasparella A, Pernigotto G, Cappelletti F, et al. Analysis and modelling of window and glazing systems energy performance for a well insulated residential building. *Energy and Building*, 2011, 43(4): 1030–1037
- Jaber S, Ajib S. Thermal and economic windows design for different climate zones. *Energy and Building*, 2011, 43(11): 3208–3215
- Dutta A, Samanta A. Reducing cooling load of buildings in the tropical climate through window glazing: a model to model comparison. *Journal of Building Engineering*, 2018, 15: 318–327
- Ihm P, Park L, Krarti M, et al. Impact of window selection on the energy performance of residential buildings in South Korea. *Energy Policy*, 2012, 44: 1–9
- Mesloub A, Ghosh A, Touahmia M, et al. Performance analysis of photovoltaic integrated shading devices (PVSDs) and semi-transparent photovoltaic (STPV) devices retrofitted to a prototype office building in a hot desert climate. *Sustainability*, 2020, 12(23): 10145
- Mesloub A, Ghosh A, Albaqawy G A, et al. Energy and daylighting evaluation of integrated semitransparent photovoltaic windows with internal light shelves in open-office buildings. *Advances in Civil Engineering*, 2020, 2020: 1–21
- Ebrahimpour A, Maerefat M. Application of advanced glazing and overhangs in residential buildings. *Energy Conversion and Management*, 2011, 52(1): 212–219
- Sherif A, El-Zafarany A, Arafa R. External perforated window solar screens: the effect of screen depth and perforation ratio on energy performance in extreme desert environments. *Energy and Building*, 2012, 52: 1–10
- Chua K J, Chou S K. Evaluating the performance of shading devices and glazing types to promote energy efficiency of residential buildings. *Building Simulation*, 2010, 3(3): 181–194

33. Palermo-Marrero A I, Oliveira A C. Effect of louver shading devices on building energy requirements. *Applied Energy*, 2010, 87(6): 2040–2049
34. Al-Saadi S N, Al-Jabri K S. Optimization of envelope design for housing in hot climates using a genetic algorithm (GA) computational approach. *Journal of Building Engineering*, 2020, 32: 101712
35. US Department of Energy. EnergyPlus energy simulation software. 2020–8–8, available at website of energyplus
36. Tuhus-Dubrow D, Krarti M. Genetic-algorithm based approach to optimize building envelope design for residential buildings. *Building and Environment*, 2010, 45(7): 1574–1581
37. Zhao J, Du Y. Multi-objective optimization design for windows and shading configuration considering energy consumption and thermal comfort: a case study for office building in different climatic regions of China. *Solar Energy*, 2020, 206: 997–1017
38. Harenberg D, Marelli S, Sudret B, et al. Uncertainty quantification and global sensitivity analysis for economic models. *Quantitative Economics*, 2019, 10(1): 1–41
39. Sheikshahrokhdehkordi M, Khalesi J, Goudarzi N. High-performance building: sensitivity analysis for simulating different combinations of components of a two-sided windcatcher. *Journal of Building Engineering*, 2020, 28: 101079
40. Alberto A, Ramos N M M, Almeida R M S F. Parametric study of double-skin facades performance in mild climate countries. *Journal of Building Engineering*, 2017, 12: 87–98
41. Ioannou A, Itard L C M. Energy performance and comfort in residential buildings: sensitivity for building parameters and occupancy. *Energy and Building*, 2015, 92: 216–233
42. Tian W. A review of sensitivity analysis methods in building energy analysis. *Renewable & Sustainable Energy Reviews*, 2013, 20: 411–419
43. Linton R, Frutiger T, Blanc S, et al. American society of heating, refrigerating and air-conditioning engineers, inc. (ASHRAE). New York, NY 1977, 1977
44. Al Busaidi A S, Kazem H A, Al-Badi A H, et al. A review of optimum sizing of hybrid PV-Wind renewable energy systems in Oman. *Renewable & Sustainable Energy Reviews*, 2016, 53: 185–193
45. Kazem H A. Renewable energy in Oman: status and future prospects. *Renewable & Sustainable Energy Reviews*, 2011, 15(8): 3465–3469
46. Climate OneBuilding Org. Climate data for building performance simulation. 2021–1, available at website of climate.onebuilding.org
47. Crawley D B, Lawrie L K, Winkelmann F C, et al. EnergyPlus: creating a new-generation building energy simulation program. *Energy and Building*, 2001, 33(4): 319–331
48. Crawley D B, Hand J W, Kummert M, et al. Contrasting the capabilities of building energy performance simulation programs. *Building and Environment*, 2008, 43(4): 661–673
49. Zhang Y. Use jEPlus as an efficient building design optimisation tool. In: CIBSE ASHRAE Technical Symposium, London, UK, 2012
50. Zhang Y. “Parallel” EnergyPlus and the development of a parametric analysis tool. International Building Performance Simulation Association, 2019
51. United States Department of Energy (DOE). EnergyPlus: Engineering Reference. California, USA 2014.
52. Kneifel J, Webb D. Life cycle cost manual for the federal energy management program. National Institute of Standards and Technology, 2020
53. Kuwait M E W. Electricity statistics year book, latest version 2019. 2020–8, available at website of mew.gov.kw
54. Cerezo C, Sokol J, AlKhaled S, et al. Comparison of four building archetype characterization methods in urban building energy modeling (UBEM): a residential case study in Kuwait City. *Energy and Building*, 2017, 154: 321–334